Occurrence frequencies of polar mesosphere summer echoes observed at 69° N during a full solar cycle

R. Latteck and J. Bremer

Leibniz Institute of Atmospheric Physics at the Rostock University, Schloss-Str. 6, 18225 Kühlungsborn, Germany

Correspondence to: R. Latteck (latteck@iap-kborn.de)

Abstract. Polar mesosphere summer echoes (PMSE) are strong enhancements of received signal power at very high radar frequencies occurring at altitudes between about 80 and 95 km at polar latitudes during summer. PMSE are caused by inhomogeneities in the electron density of the radar Bragg scale within the plasma of the cold summer mesopause region in the presence of negatively charged ice particles. Thus the occurrence of PMSE contains information about mesospheric temperature and water vapour content but also depends on the ionisation due to solar wave radiation and precipitating high energetic particles. Continuous and homogeneous observations of PMSE have been done on the North-Norwegian island Andøya (69.3° N, 16.0° E) from 1999 until 2008 using the ALWIN VHF radar at 53.5 MHz. In 2009 the Leibniz-Institute of Atmospheric Physics in Kühlungsborn, Germany (IAP) started the installation of the Middle Atmosphere Alomar Radar System (MAARSY) at the same location. The observation of mesospheric echoes could be continued in spring 2010 starting with an initial stage of expansion of MAARSY and is carried out with the completed installation of the radar since May 2011. Since both the AL-WIN radar and MAARSY are calibrated, the received echo strength of PMSE from 14 yr of mesospheric observations could be converted to absolute signal power. Occurrence frequencies based on different common thresholds of PMSE echo strength were used for investigations of the solar and geomagnetic control of the PMSE as well as of possible long-term changes. The PMSE are positively correlated with the solar Lyman α radiation and the geomagnetic activity. The occurrence frequencies of the PMSE show slightly positive trends but with marginal significance levels.

1 Introduction

The phenomenon of strong radar echoes from the mesopause region during summer is well known from VHF radar observations at frequencies between ~ 2 MHz and ~ 1 GHz at polar and middle latitudes for more than 30 yr. These so called Polar Mesosphere Summer Echoes (PMSE) are caused by inhomogeneities in the electron density of a size comparable to the radar Bragg scale (about 3 m at 50 MHz radar frequency) in the presence of negatively charged aerosol particles. At mesospheric heights under normal condition irregularities in the electron density distribution in the order of about 3 m are smoothed out by molecular diffusion (Lübken et al., 2002). Small scale structures of e.g. charged ice particles created by turbulent advection leads to similar structures in the distribution of free electrons and positive ions due to multipolar coupling between all charged species (Rapp et al., 2008). These small scale structures in the electron gas may well exist a considerable time after molecular diffusion has already destroyed any structures in the neutral gas distribution (Rapp and Lübken, 2003). First mesospheric summer echoes were observed at the end of the 1970s at mid-latitudes above the Harz mountains in Germany (Czechowsky et al., 1979) before the first echoes of this type were seen at polar latitudes above Poker Flat (Ecklund and Balsley, 1981). A detailed review about the early observations of PMSE can be found in Cho and Röttger (1997) and an overview on the current understanding of this phenomenon has been published by Rapp and Lübken (2004).

This paper gives an overview about the long-term observations of PMSE obtained with two VHF radars at the Norwegian island Andøya (69.3° N, 16.0° E) from 1999 until 2012. In contrast to earlier investigations by Bremer et al. (2006) and Bremer et al. (2009) the dependency of PMSE occurrence rates on solar and geomagnetic activity is discussed on

Table 1. Basic radar and experiment parameters relevant for volume reflectivity determination.

radar period	ALWIN 1998–2008	ALWIN64 2009	MAARSY 2010	MAARSY 2011/2012
P_t	36 kW	36 kW	250 kW	736 kW
Tx ant.	144	6	147	433
G_t	28.3 dBi	15.6 dBi	29.0 dBi	33.5 dBi
θ	6°	14.1°	6°	3.6°
Rx ant.	24	64	7	7
G_r	20.6 dBi	20.1 dBi	15.5 dBi	15.5 dBi
e	0.58	0.58	0.54	0.54
τ	300 m	300 m	210 m	210 m
$\rightarrow c_{sys}$	2.5×10^{-8}	2.3×10^{-7}	1.3×10^{-8}	4.3×10^{-9}
m	32	64	32	32
n	16	8	8	8
g_r	101 dB	107 dB	101 dB	101 dB
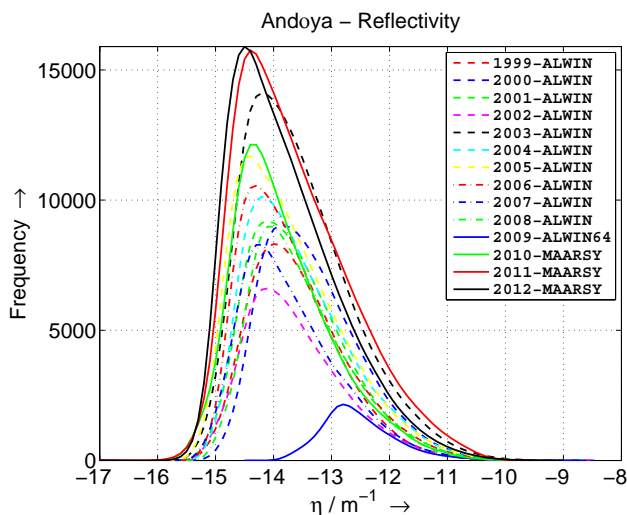
Fig. 1. Annual distributions of PMSE volume reflectivity as observed with ALWIN and MAARSY on Andøya between 1999 and 2012.

the basis of radar volume reflectivity which allows the comparison of observations from different radar systems.

2 Observation of polar mesosphere summer echoes at Andøya from 1999 until 2012

2.1 Radars used for PMSE observations

The observation of PMSE at Andøya started in the early 1990s using the mobile SOUSY radar (Czechowsky et al., 1984) and since 1994 the ALOMAR SOUSY radar (Singer et al., 1995). The latter was replaced in 1998 by the ALWIN radar (Latteck et al., 1999) which allowed unattended and remote controlled operation. After 10 yr of nearly continuous operation the ALWIN radar was switched off in September 2008 to be replaced by MAARSY (Latteck et al., 2010, 2012b) the more powerful and flexible Middle Atmosphere Alomar Radar System. Parts of the ALWIN antenna array and the container housing the transmitter and receiving units were moved approximately 100 m westward of the old radar site to be used for PMSE observation during the construction of the MAARSY antenna array in 2009. This interim solution called ALWIN64 (Latteck et al., 2010, 2012b) used six of the newly designed MAARSY antennas for transmission and 64 of the old ALWIN Yagi antennas for reception. The successive installation of MAARSY started in September 2009 upon completion of the new antenna array. The radar control and data acquisition hardware as well as 217 transceiver modules were installed in spring of 2010. A second stage of expansion to 343 transceiver modules was brought into service in November 2010 and the system was finally upgraded to 433 transceiver modules in May 2011 (Latteck et al., 2012a).

In this paper we concentrate on the period of continuous PMSE observation at Andøya starting in summer 1999 until autumn 2012, using ALWIN and MAARSY. Both radars were run at 53.5 MHz but most of the other technical parameters as e.g. the peak power P_t, the gains for the transmitting (G_t) and receiving (G_r) antennas, the antenna beam width θ and the loss factor e as well as operation parameters as e.g. the used effective pulse width τ and the number of used code elements m or the number of coherent integrations n were different. Table 1 lists the most important parameters of the used radars during the various periods of operation.

2.2 Comparability of radar observations

In order to compare PMSE occurrence rates the received echo power was converted into radar volume reflectivity which is a system independent parameter in contrast to, e.g., relative signal strength or signal-to-noise ratio, since its calculation considers the individual radar characteristics and experiment configurations. Radar volume reflectivity η is defined as the power which would be scattered if all powers were scattered isotropically with a power density equal to that of the backscattered radiation, per unit volume and per unit incident power density (Hocking, 1985). It can be expressed as

$$\eta = \frac{P_r \, 128 \, \pi^2 \, 2 ln(2) \, r^2}{P_t \, G_t \, G_r \lambda^2 \, e \, \theta_{[1/2]}^2 \, c \, \tau} \tag{1}$$

where r is the range to the scatterers, G_t and G_r are the gain of the transmitting and receiving antenna respectively, $\theta_{[1/2]}$ is the half power half-width of the transmitting antenna beam, λ is the radar wavelength, e is the system efficiency containing mainly the losses of the antenna feeding system, P_t is the transmitted peak power, P_r is the received signal power, c is the speed of light, and τ is the effective pulse width (Hocking and Röttger, 1997). The factor $2 ln(2)$ is a correction term related to the non-uniform antenna gain
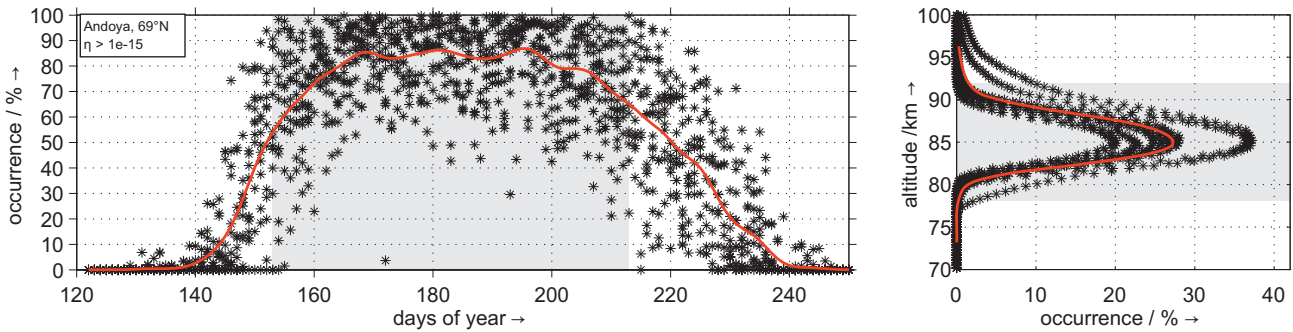
Fig. 2. Mean seasonal variation (left, thick red line) and mean height variation (right, thick red line) of PMSE occurrence rates at Andøya based on VHF-radar observations using ALWIN and MAARSY between 1999 and 2012. The star-symbols indicate the corresponding occurrence rates for the individual years. The gray shaded period and height range were used for the determination of mean PMSE occurrences for further investigation.
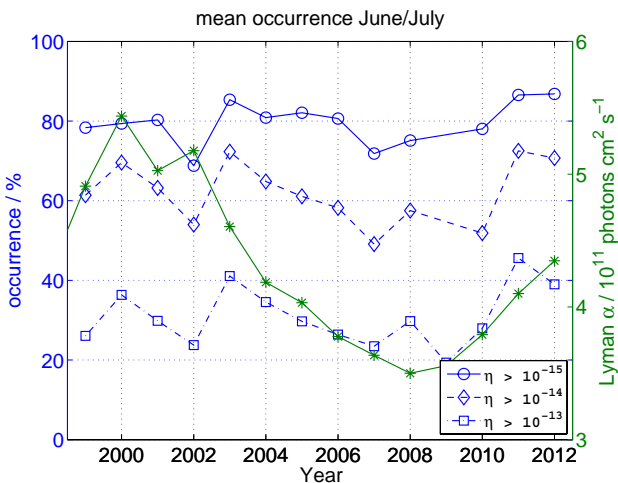

Fig. 3. Mean occurrence rates of PMSE for the months June and July from 1999 until 2012 derived from radar volume reflectivities $\eta \geq 10^{-15}$ (blue circles), $\eta \geq 10^{-14}$ (blue diamonds) and $\eta \geq 10^{-13}$ (blue squares) based on VHF-radar observations using ALWIN, ALWIN64 and MAARSY. The green stars represent the mean Lyman α values for June/July.

over the half-power beam-width (Probert-Jones, 1962; Skolnik, 1990). All system dependent parameters of Eq. (1) can be combined into a system factor c_{sys} as shown in Table 1 for the different periods and radar configurations. Hence the radar reflectivity η depends only on the range to the scatterers r and the absolute value of the received signal power P_r

$$\eta = P_r \cdot c_{sys} \cdot r^2 \qquad (2)$$

The correct determination of P_r requires the calibration of the receiving path of radar system as e.g. described in Latteck et al. (2008).

The determining of PMSE is based on 5 min averages of radar volume reflectivity. A PMSE event was defined as a radar reflectivity enhancement above the detection limit, but for a minimum duration of 20 min (i.e. 4 consecutive 5-min averages) in one range gate (Latteck et al., 2008).

Figure 1 shows the annual distribution of PMSE volume reflectivity observed with ALWIN, ALWIN64 and MAARSY on Andøya between 1999 and 2012. The left borders of the distributions illustrate the differences in sensitivity of the operational modes of the radars, most convincingly shown by the solid blue line representing the ALWIN64 observations in 2009. The differences in echo detection sensitivity is also represented in the absolute values of the peaks of the distribution of the various years. This parameter is also predominantly affected by the annual variation of PMSE occurrence caused by geophysical variations, as can clearly be seen by comparing e.g. the dashed curves representing ALWIN results only.

2.3 Long term changes in PMSE occurrence rates

A qualitative comparison of the PMSE occurrence rates of the various years required the consideration of even marginal small differences in echo detecting sensitivity due to system and operational differences of the radars. Therefore a minimum value $\eta_{min} = 10^{-15}$ m^{-1} was defined and occurrence rates were calculated for PMSE greater than this threshold for all the year between 1999 and 2012. The left plot in Fig. 2 illustrates the results as daily values (black stars) of the individual years and a polynomial fit (red line) through the corresponding daily averages. The characteristic of the derived mean seasonal variation of PMSE is similar to the results found earlier by Bremer et al. (2009). Here, however, the start of the season is 4 days earlier near 16 May.

For the further study of long term changes in PMSE occurrence rates the possible influence of ionisation caused by solar and geomagnetic activity have been investigated following the procedure used by Bremer et al. (2009). Seasonal mean values of PMSE for the time period from 1 June until 31 July and the height range between 78.5 and 92 km (gray shaded areas in Fig. 2) have been calculated for every year

and compared with corresponding mean values of the solar Lyman α radiation and of the geomagnetic Ap index. The Lyman α radiation is the dominant ionisation source (ionisation of nitric oxide) in the undisturbed ionospheric D region whereas the geomagnetic Ap index may be an indicator for precipitating high energetic particle flux (Bremer et al., 2009). Since the echo detection sensitivity for ALWIN64 in 2009 was extremely lower compared to the other years, two more sets of PMSE occurrence rates for the individual years were derived using thresholds of $\eta_{min} = 10^{-14}$ m^{-1} and $\eta_{min} = 10^{-13}$ m^{-1}. The latter allowed to include the 2009 observations in the study. Figure 3 shows the corresponding PMSE occurrence rates OR_{-15}, OR_{-14} and OR_{-13} derived for the three thresholds $\eta \geq 10^{-15}$ m^{-1} (blue circles), $\eta \geq 10^{-14}$ m^{-1} (blue diamonds) and $\eta \geq 10^{-13}$ m^{-1} (blue squares) respectively. The green stars are the mean Lyman α values for June/July representing mean solar activity during the last solar cycle. All three occurrence rate series show a similar behavior with slight variations but on different levels and indicate no obvious dependence on the solar cycle.

Qualitative results of the dependency of three PMSE occurrence rates OR_{-15}, OR_{-14} and OR_{-13} on the solar Lyman α radiation as well as on the geomagnetic Ap index are shown in the left, middle and right plots of the upper and middle panels of Fig. 5, respectively. The correlation between Lyman α and the PMSE occurrence rates OR_{-15} representing most echoes is slightly negative, whereas a positive correlation with Lyman α is given for OR_{-14} (middle panel) and OR_{-13} (right panel). A general positive correlation exists in the comparison of all three PMSE series with Ap, indicating an increasing PMSE occurrence with increasing ionisation level caused by enhanced geomagnetic activity.

The influence of both parameters on the PMSE occurrence has been removed by a twofold regression analysis

$$OR' = a + b \cdot Ly\,\alpha + c \cdot Ap \qquad (3)$$

following the procedure described in Bremer et al. (2009) in order to investigate possible long-term variations of PMSE. The differences ΔOR_{-15}, ΔOR_{-14} and ΔOR_{-13} between the original observed occurrence rates OR_{-15}, OR_{-14} and OR_{-13} and the adjusted occurrences rates OR' are shown in the three plots of the lower panel of Fig. 5, respectively. An estimated linear trend line shows a slightly positive trend of $0.39 \pm 0.67\%/a$, $0.52 \pm 0.83\%/a$ and $0.64 \pm 0.78\%/a$ for ΔOR_{-15}, ΔOR_{-14} and ΔOR_{-13}, respectively. The error values of the different trends have been estimated for a significance level of 95 %. As can be seen for all trends that the correct significance levels are smaller than 95 % (77 %, 80 %, 90 %).

3 Discussion

The present study was conducted to update earlier investigations (Bremer et al., 2006, 2009) with data series obtained
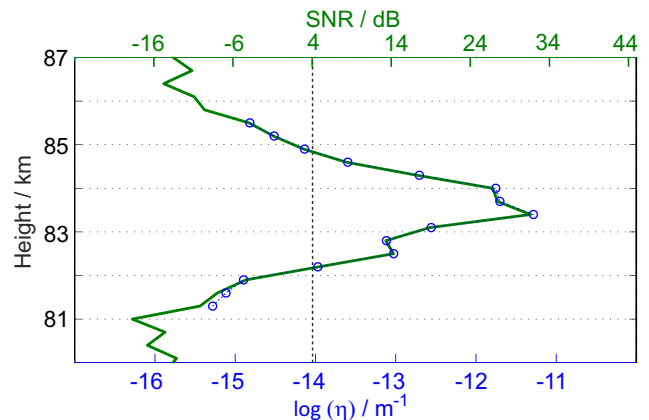

Fig. 4. Height profile (10 min average) of a PMSE obtained on 15 July 2008 at 12:00 UT using ALWIN shown as signal-to-noise ratio (green line) as well as volume reflectivity (blue dashed line and circles). The vertical black dashed line shows the connection between the threshold as used in Bremer et al. (2009) for ALWIN data and the corresponding value in volume reflectivity.

at the same location but with the more powerful and flexible Middle Atmosphere Alomar Radar System (MAARSY). In contrast to these earlier studies the PMSE occurrence rates were derived on the basis of radar volume reflectivity using a common threshold instead of using several SNR-thresholds adjusted to the system parameters. This allows a more flexible comparison of observations from different radar systems as once the received echo power is converted into reflectivity various thresholds can easily be chosen in order to consider the different PMSE detection limits of the various radars based on differences in system parameters and experiment configurations as shown in Fig. 1.

Three common thresholds of volume reflectivity OR_{-15}, OR_{-14} and OR_{-13} have been used to investigate the dependence of PMSE occurrence on solar and geomagnetic activity. The results are presented in the upper and middle panels of Fig. 5. The correlation between Lyman α and PMSE occurrence rates OR_{-15} (Fig. 5, left top plot) representing all detected echoes is slightly negative whereas a positive correlation with Lyman α is given for OR_{-14} (Fig. 5, middle top plot) and OR_{-13} (Fig. 5, right top plot) both representing well pronounced echoes only. The latter also eliminate daily variations on PMSE occurrence due to daily variation of background noise. Furthermore OR_{-14} is very comparable with the SNR-threshold as used in Bremer et al. (2009) for ALWIN data as shown in Fig. 4. The results indicate a generally low dependence of PMSE occurrence on solar activity and also confirms the conclusion by Bremer et al. (2009) that various processes caused by solar radiation, reduce the influence of increasing electron density due to increasing ionisation which actually should increase PMSE.

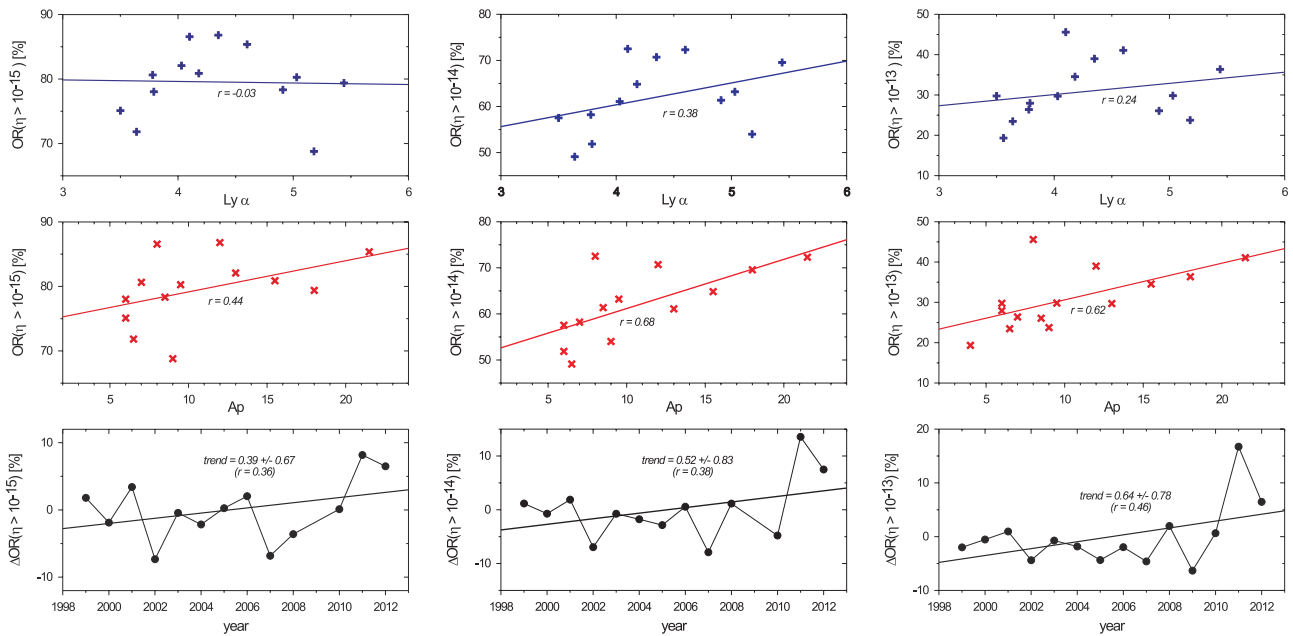The correlation found between the PMSE occurrence series and the geomagnetic activity represented by Ap was

Fig. 5. Dependence of the PMSE occurrence rates OR_{-15} (left panels), OR_{-14} (middle panels) and OR_{-13} (right panels) on the solar Lyman α radiation (upper panels) and on geomagnetic Ap index (middle panels) as well as long-term variation of the PMSE occurrence rates after elimination of their solar and geomagnetically caused parts (lower panels).

positive for OR_{-15} (Fig. 5, left middle plot), OR_{-14} (Fig. 5, center plot) as well as for OR_{-13} (Fig. 5, right middle plot). This is an indication for a direct influence of precipitating fluxes of high energetic particles to the increase of electron densities and therefore the increase of PMSE occurrence. The PMSE trends in the lower part of Fig. 5 are for all three investigated thresholds of volume reflectivity positive with significance levels between about 77–90 %.

4 Summary and conclusion

Polar mesospheric summer echoes from 14 yr of continuous VHF radar observations at Andøya (69° N) have been investigated for solar and geomagnetic control as well as for possible long-term changes. The investigation is based on occurrence rates derived from radar volume reflectivity of the received echoes considering the differences in technical performance and experimental operation of the radars ALWIN and MAARSY used at the same site during the long period of observation. The given differences in detection sensitivity of the used radars were taken into account by using various common thresholds of PMSE echo strength for the determination of the occurrence frequencies.

The correlation of PMSE occurrence with the solar Lyman α radiation depends on the applied threshold for the detection of PMSE. A positive correlation is only seen if well pronounced echoes are taken into account. Nevertheless the results confirm the conclusion by Bremer et al. (2009) that various processes caused by solar radiation reduce the influ-

ence of increasing electron density due to increasing ionisation which should actually increase PMSE.

A significant correlation between the PMSE occurrence rate and the geomagnetic activity represented by Ap was found independently of the used PMSE detection thresholds, confirming the direct influence of precipitating fluxes of high energetic particles to the increase of electron densities and therefore the increase of PMSE.

After eliminating the influences of solar and geomagnetic activity, the PMSE occurrence frequencies show slightly positive trends but with small significance levels. The latter is probably caused by the short period of observation of 14 yr.

Future activities will be directed to the integration of PMSE data from earlier years obtained with the ALOMAR SOUSY radar between 1994 and 1997. Since ALWIN data can be directly converted from SNR into volume reflectivity and vice versa as illustrated in Fig. 4, the ALWIN data set could be used to adjust the older (SOUSY) and newer (MAARSY) data to a common threshold for long term investigation of PMSE occurrence rates. This will improve the overall data availability and should also improve the significance of the trends.

References

Bremer, J., Hoffmann, P., Höffner, J., Latteck, R., Singer, W., Zecha, M., and Zeller, O.: Long-term changes of mesospheric summer echoes at polar and middle latitudes, J. Atmos. Solar Terr. Phys., 68, 1940–1951, doi:10.1016/j.jastp.2006.02.012, 2006.

Bremer, J., Hoffmann, P., Latteck, R., Singer, W., and Zecha, M.: Long-term changes of (polar) mesosphere summer echoes, J. Atmos. Solar-Terr. Phys., 71, 1571–1576, doi:10.1016/jastp.2009.03.010, 2009.

Cho, J. Y. N. and Röttger, J.: An updated review of polar mesosphere summer echoes: Observation, theory, and their relationship to noctilucent clouds and subvisible aerosols, J. Geophys. Res., 102, 2001–2020, 1997.

Czechowsky, P., Rüster, R., and Schmidt, G.: Variations of mesospheric structures in different seasons, Geophys. Res. Lett., 6, 459–462, 1979.

Czechowsky, P., Schmidt, G., and Rüster, R.: The mobile SOUSY Doppler radar: Techical design and first results., Radio Sci., 19, 441–450, 1984.

Ecklund, W. L. and Balsley, B. B.: Long-term observations of the Arctic mesosphere with the MST radar at Poker Flat, Alaska, J. Geophys. Res., 86, 7775–7780, 1981.

Hocking, W. K.: Measurements of turbulent energy dissipation rates in the middle atmosphere by radar techniques: A review, Radio Sci., 20, 1403–1422, 1985.

Hocking, W. K. and Röttger, J.: Studies of polar mesosphere summer echoes over EISCAT using calibrated signal strengths and statistical parameters, Radio Sci., 32, 1425–1444, 1997.

Latteck, R., Singer, W., and Bardey, H.: The ALWIN MST radar – Technical design and performances, in: Proceedings of the 14th ESA Symposium on European Rocket and Balloon Programmes and Related Research, Potsdam, Germany (ESA SP–437), edited by Kaldeich-Schürmann, B., 179–184, 1999.

Latteck, R., Singer, W., Morris, R. J., Hocking, W. K., Murphy, D. J., Holdsworth, D. A., and Swarnalingam, N.: Similarities and differences in polar mesosphere summer echoes observed in the Arctic and Antarctica, Ann. Geophys., 26, 2795–2806, doi:10.5194/angeo-26-2795-2008, 2008.

Latteck, R., Singer, W., Rapp, M., and Renkwitz, T.: MAARSY – The new MST radar on Andøya/ Norway, Adv. Radio Sci., 8, 219–224, doi:10.5194/ars-8-219-2010, 2010.

Latteck, R., Singer, W., Rapp, M., Renkwitz, T., and Stober, G.: Horizontally resolved structures of radar backscatter from polar mesospheric layers, Adv. Radio Sci., 10, doi:10.5194/ars-10-1-2012, 2012a.

Latteck, R., Singer, W., Rapp, M., Vandepeer, B., Renkwitz, T., Zecha, M., and Stober, G.: MAARSY – The new MST radar on Andøya: System description and first results, Radio Sci., 47, RS1006, doi:10.1029/2011RS004775, 2012b.

Lübken, F.-J., Rapp, M., and Hoffmann, P.: Neutral air turbulence and temperatures in the vicinity of polar mesosphere summer echoes, J. Geophys. Res., 107, 4273, doi:10.1029/2001JD000915, 2002.

Probert-Jones, J. R.: The Radar Equation in Meteorology, Q. J. Roy. Meteorol. Soc., 88, 485–495, 1962.

Rapp, M. and Lübken, F.-J.: On the nature of PMSE: Electron diffusion in the vicinity of charged particles revisited, J. Geophys. Res., 108, 8437, doi:10.1029/2002JD002857, 2003.

Rapp, M. and Lübken, F.-J.: Polar mesosphere summer echoes (PMSE): Review of observations and current understanding, Atmos. Chem. Phys., 4, 2601–2633, doi:10.5194/acp-4-2601-2004, 2004.

Rapp, M., Strelnikova, I., Latteck, R., Hoffmann, P., Hoppe, U.-P., Häggström, I., and Rietveld, M. T.: Polar mesosphere summer echoes (PMSE) studied at Bragg wavelengths of 2.8 m, 67 cm, and 16 cm, J. Atmos. Solar-Terr. Phys., 70, 947–961, doi:10.1016/j.jastp.2007.11.005, 2008.

Singer, W., Keuer, D., Hoffmann, P., Czechowsky, P., and Schmidt, G.: The ALOMAR SOUSY radar: Technical design and further developments, in: Proceedings of the 12th ESA Symposium on European Rocket and Balloon Programmes and Related Research, Lillehammer, Norway (ESA SP–370), 409–415, 1995.

Skolnik, M.: Radar handbook, McGraw-Hill, 1990.